



Since January 2020 Elsevier has created a COVID-19 resource centre with free information in English and Mandarin on the novel coronavirus COVID-19. The COVID-19 resource centre is hosted on Elsevier Connect, the company's public news and information website.

Elsevier hereby grants permission to make all its COVID-19-related research that is available on the COVID-19 resource centre - including this research content - immediately available in PubMed Central and other publicly funded repositories, such as the WHO COVID database with rights for unrestricted research re-use and analyses in any form or by any means with acknowledgement of the original source. These permissions are granted for free by Elsevier for as long as the COVID-19 resource centre remains active.

Journal Pre-proof

A comparative study of 5- fluorouracil, doxorubicin, methotrexate, paclitaxel for their inhibition ability for Mpro of nCoV: Molecular docking and molecular dynamics simulations

Madhur Babu Singh, Vijay Kumar Vishvakarma, Aditya Aryan Lal, Ramesh Chandra, Pallavi Jain, Prashant Singh

PII: S0019-4522(22)00452-6

DOI: <https://doi.org/10.1016/j.jics.2022.100790>

Reference: JICS 100790

To appear in: *Journal of the Indian Chemical Society*

Received Date: 10 June 2022

Revised Date: 7 October 2022

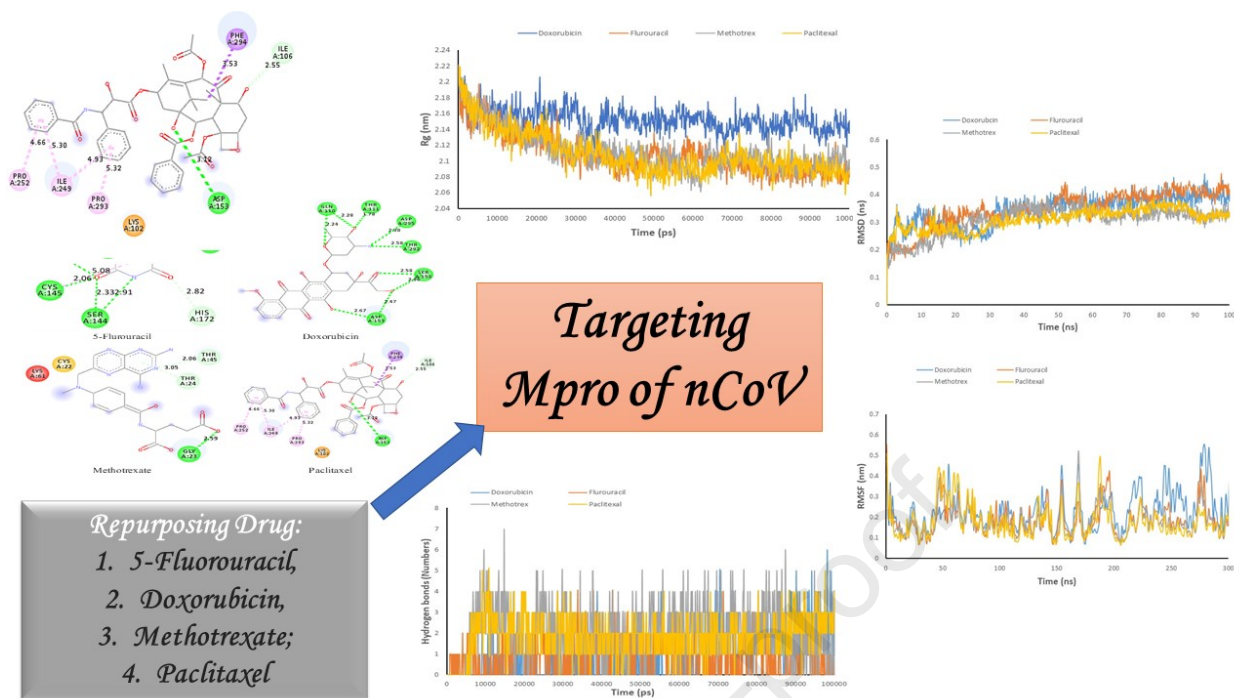
Accepted Date: 29 October 2022

Please cite this article as: M.B. Singh, V.K. Vishvakarma, A.A. Lal, R. Chandra, P. Jain, P. Singh, A comparative study of 5- fluorouracil, doxorubicin, methotrexate, paclitaxel for their inhibition ability for Mpro of nCoV: Molecular docking and molecular dynamics simulations, *Journal of the Indian Chemical Society* (2022), doi: <https://doi.org/10.1016/j.jics.2022.100790>.

This is a PDF file of an article that has undergone enhancements after acceptance, such as the addition of a cover page and metadata, and formatting for readability, but it is not yet the definitive version of record. This version will undergo additional copyediting, typesetting and review before it is published in its final form, but we are providing this version to give early visibility of the article. Please note that, during the production process, errors may be discovered which could affect the content, and all legal disclaimers that apply to the journal pertain.

© 2022 Indian Chemical Society. Published by Elsevier B.V. All rights reserved.





A Comparative Study of 5- Fluorouracil , Doxorubicin, Methotrexate, Paclitaxel for their Inhibition ability for Mpro of nCoV: Molecular Docking and Molecular Dynamics Simulations

Madhur Babu Singh,^{1,2} Vijay Kumar Vishvakarma,¹ Aditya Aryan Lal,² Ramesh Chandra,^{3,*} Pallavi Jain,^{4,*} Prashant Singh^{1,*}

¹Department of Chemistry, Atma Ram Sanatan Dharma College, University of Delhi, Delhi, India;

²Department of Physics & Electronics, Hansraj College, University of Delhi, Delhi, India;

³Department of Chemistry, University of Delhi, Delhi, India;

⁴Department of Chemistry, Faculty of Engineering and Technology, SRM Institute of Science and Technology, Delhi-NCR Campus, Uttar Pradesh, India

*Corresponding author

Email: acbrdu@hotmail.com; palli24@gmail.com & psingh@arsd.du.ac.in

Abstract

A new corona virus (nCoV) is aetiological agent responsible for the viral pneumonia epidemic. There is no specific therapeutic medicines available for the treatment of this condition and also effective treatment choices are few. In this work author tried to investigate some repurposing drug such as 5- fluorouracil, doxorubicin, methotrexate and paclitaxel against the main protease (Mpro) of nCoV by the computational model. Molecular docking was performed to screen out the best compound and doxorubicin was found to have minimum binding energy -121.89 kcal/mol. To further study, MD simulations were performed at 300 K and the result successfully corroborate the energy obtained by molecular docking. Temperature dependent MD simulation of the best molecule that is doxorubicin obtained from docking result was performed to check the variation in structural changes in Mpro of nCoV at 290 K, 310 K, 320 K and 325 K. It is sound that doxorubicin binds effectively with Mpro of nCoV at 290 K. Further ADME properties of the 5- fluorouracil, doxorubicin, methotrexate and paclitaxel were also evaluated to understand the bioavailability.

Keywords: Mpro of nCoV; Molecular dynamics simulations; Molecular docking; ADME

Introduction

The new public health crisis is threatening the world in December 2019 with the spread of novel Corona. This disease is spread by the inhalation of the droplet from the infected person that shows the symptoms around 2 to 14 days. The genome of a coronavirus is comprised of a single strand of positive-sense RNA, and it is encased in a membrane envelope. CoV are rather massive viruses. The crown-like look that coronaviruses have is due to the presence of glycoprotein spikes that are embedded in the viral membrane.¹ There are four different classes of coronaviruses, which are denoted by the letters alpha, beta, gamma, and delta, respectively. The severe acute respiratory syndrome coronavirus (SARS-CoV), the middle east respiratory syndrome coronavirus (MERS-CoV), and the recently found severe acute respiratory syndrome coronavirus 2 are all members of the beta-coronavirus class (SARS-CoV-2)². Although it is part of the beta-coronaviruses category, the SARS-CoV-2 virus is distinct from both the MERS-CoV and the SARS-CoV strains. There have been reports that the genes of SARS-CoV-2 contain fewer than 80% of the same nucleotides as those of SARS-CoV, and that this virus is more contagious than previous SARS-CoV viruses³.

The genome of the SARS-CoV-2 virus is made up of around 30,000 nucleotides. The glycosylated spike protein (S), envelope protein (E), membrane protein (M), and nucleocapsid protein are some of the structural proteins that it encodes (N). In addition, the genome of the virus encodes a large number of proteins that are not structural, such as RNA-dependent RNA polymerase (RdRp), Mpro, and papain-like protease (PLpro).⁴ The viral genome is released when it has successfully entered the host cell, and it is then translated into viral polyproteins by the translation machinery found in the host cell.⁵ After then, the viral proteases PLpro and Mpro cleave the poly-proteins into effector proteins. The Mpro, which is also referred to as 3-chymotrypsin-like protease (3CL), is an enzyme that is essential to the mechanism by which the virus replicates itself. It does this by cleaving the pp1a and pp1b polyproteins, which then results in the release of functional proteins such as RNA polymerase, endoribonuclease, and exoribonuclease. As a result, Mpro is a candidate for investigation as a screening target for anti-coronaviruses. In fact, putting a halt to the activities of Mpro might prevent the infection from spreading.⁶ The symptoms are fever, cold, cough, chills, breathlessness, fatigue, and sore throat. This disease is mild for some peoples but those having the comorbidities, causes Pneumonia (Severe acute respiratory syndrome) and organ damage.⁷⁻⁹ The second wave of SARS-COV-2 causes more fatality in India

due to the shortage of oxygen and medical supports. The second wave virus is the mutant virus having additional symptoms like vomiting, diarrhoea and clotting problems.¹⁰ Peoples with severe COVID-19 is treated with remdesivir with a 10-day course while those patients with severe COVID-19 with hypoxia and require oxygen support but don't require ventilator support can come out of danger within 5-10 days of remdesivir.¹¹ Advancement in the computational tools in drug discovery is expanding for the drug discovery. Molecular docking is used to find the binding affinity of small ligands against the receptor.^{12,13} it aims is to obtained ligand-receptor complex formation with the best optimized conformation possess less binding energy¹⁴⁻¹⁶

Molecular dynamics (MD) is a computational approach used for predicting the changes in coordinates of atoms and molecules of target. The atoms and molecules are allowed to interact for a fixed period of time, giving a view of the dynamic evolutions of the complex.^{17,18} In this approach, the dynamic model is under the force of motion to be investigated. This motion of the stimulation can be studied by a different numerical solution like classical Newtonian dynamic equations, that gives the information about the atom's sites in the molecule along with the thermodynamic properties of the molecules.¹⁹ 5- fluorouracil is the generic trade name drug called adrucil. It is an anticancer chemotherapeutic drug and it is classified as an anti-metabolite. It can be used for the treatment of colon, anal, Breast, cervical, bladder, Gastrointestinal cancers.^{20,21} Doxorubicin is a member of the anthracycline antibiotic class. It stops the growth of cancerous cells by inhibiting the enzyme called topo-isomerase2.^{22,23} Doxorubicin also forms oxygen free radicals that causes the cytotoxicity secondary to lipid peroxidation of cell membrane lipids.^{24,25} Methotrexate is also known as amethopterin drug, is an anti- cancerous drugged immune system suppressant. They can be used to treat cancers, auto-immune diseases, ectopic pregnancies, medical abortions, rheumatoid arthritis etc.^{26,27} Paclitaxel is an anti-cancerous drug and sold as Taxol in treatment of cancers.²⁸ The cells treated by the paclitaxel having defects in mitotic spindle, chromosome segregation and cell division.^{29,30} In the present work, authors have taken four biological potent molecules, 5-fluorouracil, doxorubicin, methotrexate, paclitaxel and docked them against the Mpro of nCoV using iGemdock. Then, ADMET of these molecules is determined. Further, the MD simulations of 5-fluorouracil, doxorubicin, methotrexate, paclitaxel against the Mpro of nCoV are performed to understand the structural change in the Mpro of nCoV in presence of molecules.

Theoretical calculations

Designing of ligands

Herein, the ligands (5-fluorouracil, doxorubicin, methotrexate, and paclitaxel) are drawn using chemdraw³¹ as in **Figure 1**.

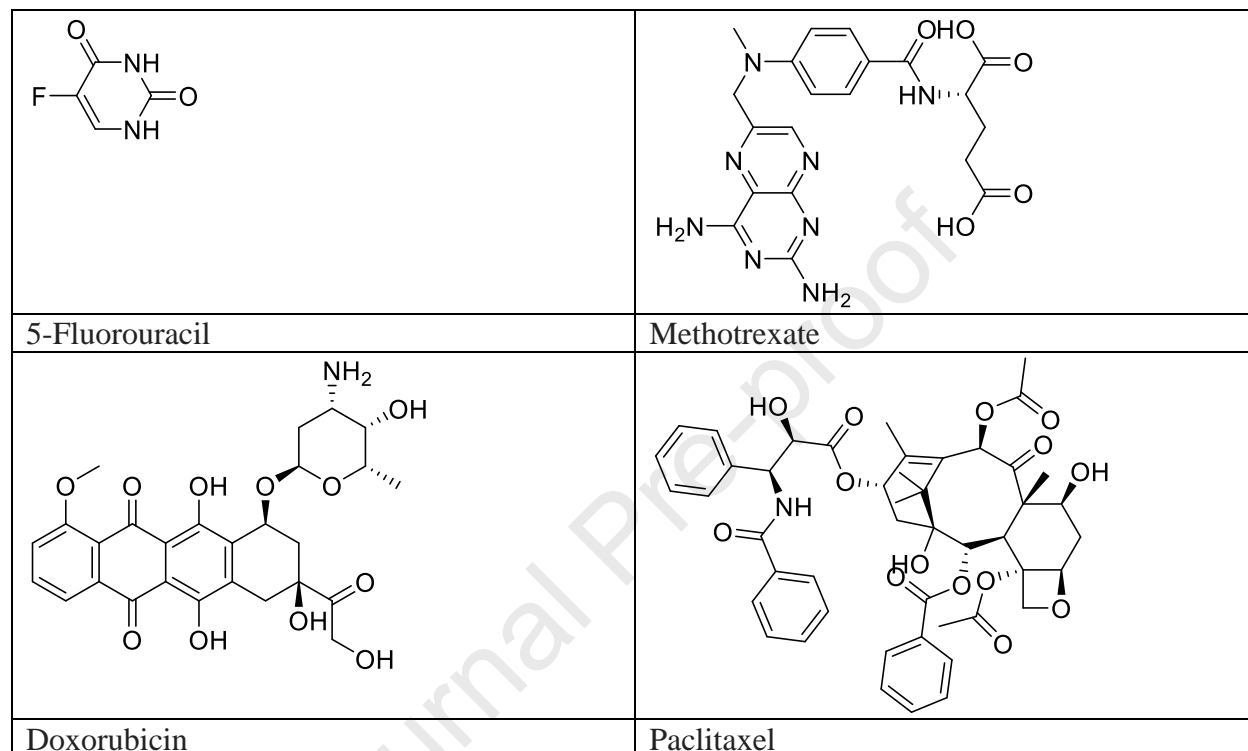


Figure 1 Structures of 5-fluorouracil, doxorubicin, methotrexate, paclitaxel

Molecular docking

Before performing the molecular docking, there is a need to do the preparation of ligands (5-fluorouracil, doxorubicin, methotrexate, paclitaxel) and (Mpro of nCoV). The crystal structure of Mpro of nCoV is downloaded from RCSB (PDB:6LU7) (<https://www.rcsb.org/structure/6LU7>). Then pdb was open in Molegro Molecular Viewer where heteroatom, ligand and water molecules were deleted. The addition of hydrogen atoms and charges in the Mpro of nCoV have been done using chimera.³²⁻³⁴ Further, the ligands were optimized by applying MM2 in Chemdraw to set the orientation of molecules for docking. The molecules were then docked using iGemdock and studied based on the binding energy (kcal/mol), obtained due to electrostatic interactions, van der Waal's. interactions and hydrogen bonding as in **Table 1**.^{35,36} Herein the allosteric binding cavity search method was used to find both an effective candidate and a novel allosteric cavity in the

receptor.³⁷ **Table 1** shows the docking results in term of energy for 5-fluorouracil, doxorubicin, methotrexate and paclitaxel against Mpro of nCoV and the binding energies of these compounds are -74.5918, -121.89, -111.43, and -99.9097 kcal /mol respectively. From these energies we conclude that doxorubicin has minimum energy, and it shows the best interaction with Mpro of nCoV.

Table 1 Biding energy of the 5-fluorouracil, doxorubicin, methotrexate, paclitaxel with Mpro of nCoV using iGemdock

S.No.	Compound	Binding Energy (kcal /mol)	Evdw (kcal /mol)	EHBond (kcal /mol)
1	5-Fluorouracil	-74.5918	-45.2049	-29.3869
2	Doxorubicin	-121.89	-79.0216	-42.8679
3	Methotrexate	-111.43	-71.2463	-40.1839
4	Paclitaxel	-99.9097	-89.286	-10.6237

Figure 2 shows the docked poses of 5-fluorouracil, doxorubicin, methotrexate and paclitaxel against the Mpro of nCoV. The 5-Fluorouracil clearly show classical hydrogen bonding interaction with GLY143, CYS145 and SER144 with distances of 2.89, 2.06 and 2.91 Å respectively and non-classical hydrogen bonding with HIS172 and ASN142 with distances of 2.82 and 3.29 Å respectively. It also shows hydrophobic interaction with CYS145 at distance of 5.08 Å. The doxorubicin shows classical hydrogen bonding interaction with GLN110, THR111, ASP295, THR292, SER158 and ASP153 with distances of 2.28, 1.78, 2.98, 2.58, 2.66 and 2.47 Å respectively and non-classical hydrogen bonding with SER158 at distance of 2.48 Å. Methotrexate exhibits classical hydrogen bonding with GLY23 with distance of 2.59 Å and non-classical hydrogen bonding with THR45 and LYS24 at distances of 2.06 and 3.05 Å respectively. The paclitaxel shows classical hydrogen bonding interaction with ASP153 at distance of 3.12 Å and non-classical hydrogen bonding interaction with ILE106 at distance of 2.55 Å. There are four hydrophobic interactions of paclitaxel with PRO252, ILE249, PRO293 and PHE294 with distances of 4.66, 5.30, 5.32 and 5.53 respectively as given in **Table 2**.

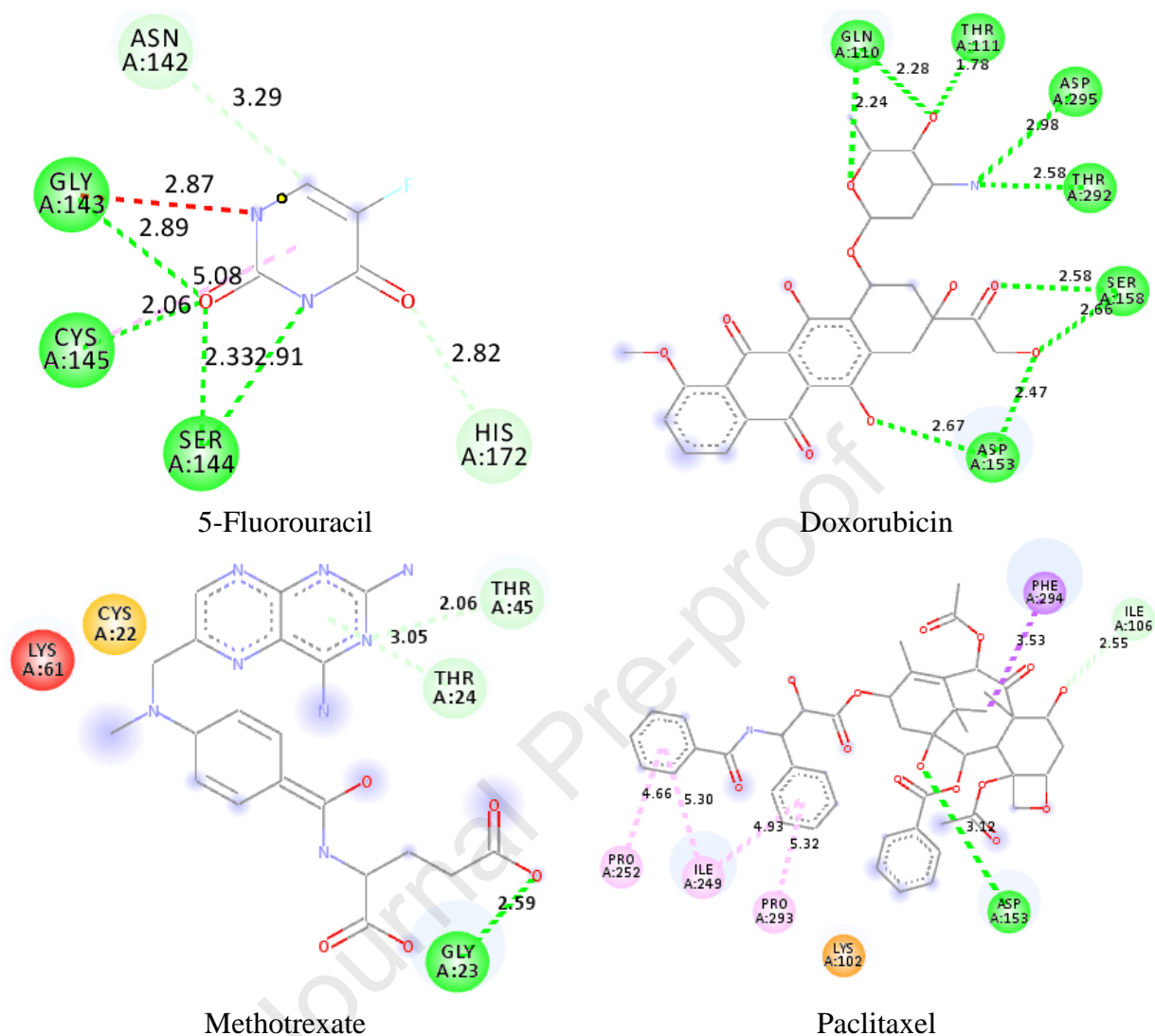


Figure 2 Two dimensional docked views of 5-fluorouracil, doxorubicin, methotrexate and paclitaxel with Mpro of nCoV

Table 2 Different types of interaction of 5-fluorouracil, doxorubicin, methotrexate and Paclitaxel with Mpro of nCoV

Ligand	H-Bond				Hydrophobic	
	Classical		Non-classical		Amino Acid	Distance
	Amino Acid	Distance	Amino Acid	Distance		
5-Fluorouracil	GLY143	2.89	HIS172	2.82	CYS145	5.08
	CYS145	2.06	ASN142	3.29		
	SER144	2.33, 2.91				
Doxorubicin	GLN110	2.24, 2.28	SER158	2.48		

	THR111	1.78				
	ASP295	2.98				
	THR292	2.58				
	SER158	2.58, 2.66				
	ASP153	2.67, 2.47				
Methotrexate	GLY23	2.59	THR45	2.06		
			LYS24	3.05		
Paclitaxel	ASP153	3.12	ILE106	2.55	PRO252	4.66
					ILE249	5.30, 4.93
					PRO293	5.32
					PHE294	5.53

Molecular Dynamics (MD) simulations

WebGro (<https://simlab.uams.edu/>) was used to perform the molecular dynamic simulation and it uses the GROMACS simulation program. Before performing MD simulations topology of ligand was generated using The GlycoBioChem PRODRG2 Server (<http://davapc1.bioch.dundee.ac.uk/cgi-bin/prodrg>). Then pdb of Mpro of nCoV and ligand topology in zip format was put on server Herein, the forcefield used is GROMACS96 43a1, water model is SPC, box type is triclinic, salt type is NaCl. Equilibration type NVT/NPT and MD run parameters used are pressure 1 bar, temperature 300 K, simulation time 100 ns and number of frames per simulation 1000.³⁸⁻⁴² Further temperature dependent (290, 310, 320, 325K) MD simulations of molecules (doxorubicin) having minimum binding energy is carried out to check the potential of doxorubicin against Mpro of nCoV. Molecular dynamic (MD) simulations is one the realistic technique which extensively used to characterize the macromolecular system. It provides the information for stability of conformational changes at the precision of nanosecond level. It allows system to show the changes at the precision of the atomic level in term of coordinates.^{43,44} It is based on the classical mechanics and easy to use. It provides the trajectories coordinates of the macromolecular system and based on this coordinates hydrogen bonding, root mean square fluctuation (RMSF), root mean square deviation (RMSD) and radius of gyration were calculated and analyzed.⁴⁵ The docked view obtained from MD simulations at 1000 number of frame per simulation is given in **Figure 3**.

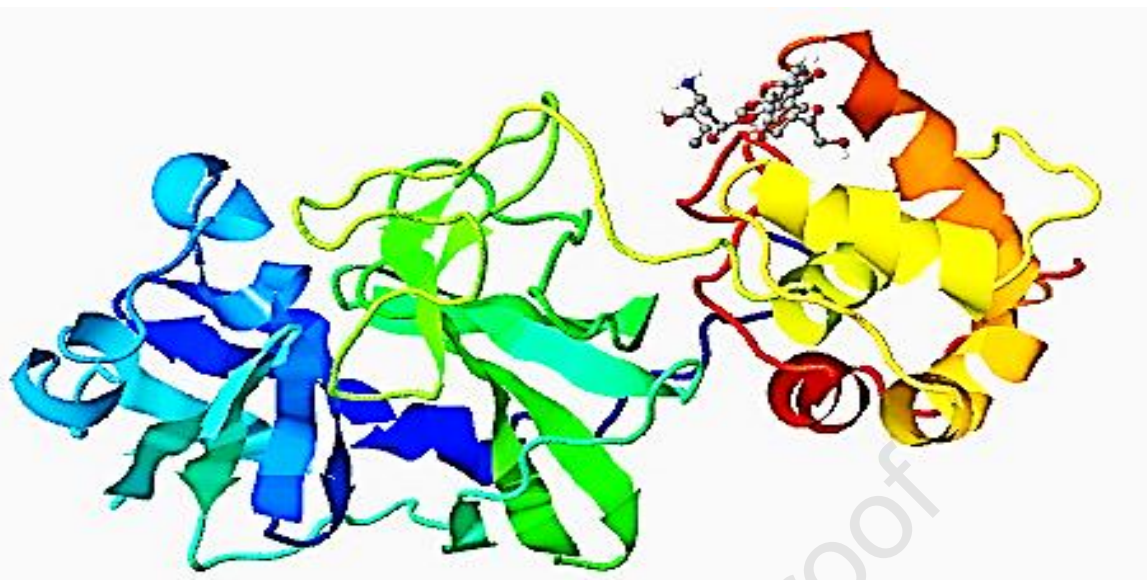


Figure 3 Docked view of the promising doxorubicin against Mpro of nCoV at 300 K

The distance from the centre of mass of a body to the point at which the mass of the body might be concentrated without causing a change in its moment of rotational inertia around an axis that passes through the centre of mass is referred to as the radius of gyration. It shows the compactness of the system and explains the conformational stability. When ligand is induced fit into the active binding cavity of the macromolecular system, the conformational changes occur in it.⁴⁶ These conformational changes can be optimized in term of radius of gyration. The overall lesser value of Rg indicates the compact nature of the molecule while the irregularity at any particular point indicates the conformational instability at that point. Herein, radius of gyration analysis for the Mpro of nCoV in the presence of 5-fluorouracil, doxorubicin, methotrexate and paclitaxel were analyzed for 100 ns at 300 K as given in **Figure 4**. The average value of Rg for 5-Fluorouracil, Methotrexate and Paclitaxel were found near 2.1 nm while for the Doxorubicin at 2.15 nm. This result indicates that the 5-fluorouracil, methotrexate, paclitaxel and doxorubicin showed similar stability of their complexes. No major fluctuation is recorded in the values of Rg during the 100 ns time span. It indicates the conformational stability of the formed complex between SARS-CoV-2 with 5-fluorouracil, doxorubicin, methotrexate and paclitaxel. During the 100 ns time span, the system shows more conformational stability as the Rg values tends to decrease

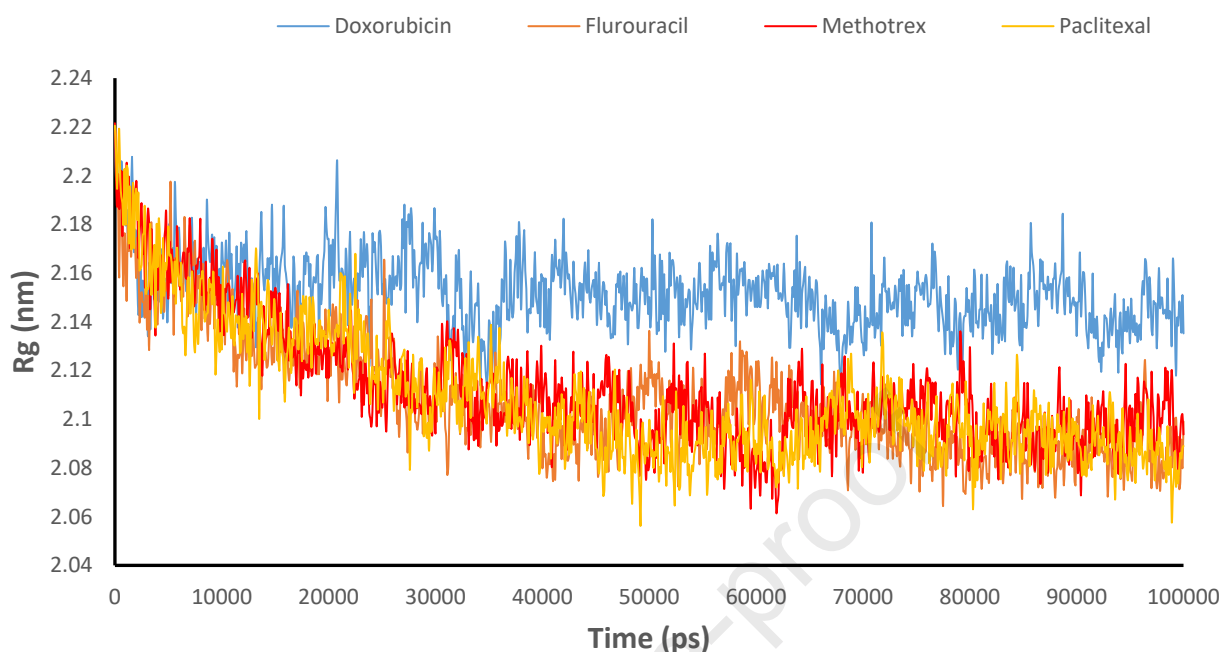


Figure 4 Trajectory of radius of gyration for the main protease of SARS-CoV-2 with 5-fluorouracil, doxorubicin, methotrexate and paclitaxel at 300 K

Root mean square deviation (RMSD) is the physical parameter to express the changes in atomic coordinates. Calculating the RMSD of proteins permits the quantification of the degree of conformational changes that occur during MD simulations. These RMSD values for the system can be used to analyse the conformational stability of the main protease of SARS-Cov-2 in presence of designed ligand. Coordinates of the backbone atoms were retrieved from the trajectory points obtained from the MD simulations. When ligand is induced fit into the active binding cavity of the main protease of SARS-CoV-2, the coordinates of the backbone atoms get disturbed the same is reflected in term of RMSD.⁴⁷ Small or minor changes in RMSD values are permissible, however, major changes leads to the conformational instability of target.⁴⁸ Herein, RMSD analysis for the main protease of SARS-CoV-2 with 5-fluorouracil, doxorubicin, methotrexate and paclitaxel were analysed for 100 ns at 300 K (**Figure 5**). In case of methotrexate and paclitaxel the RMSD values were ranges near 0.3 nm while in case of 5-fluorouracil and doxorubicin it ranges near 0.35 nm. RMSD value shows constant slight increase without any major fluctuation indicate some conformational instability towards the 100 ns time span and are on acceptable range.

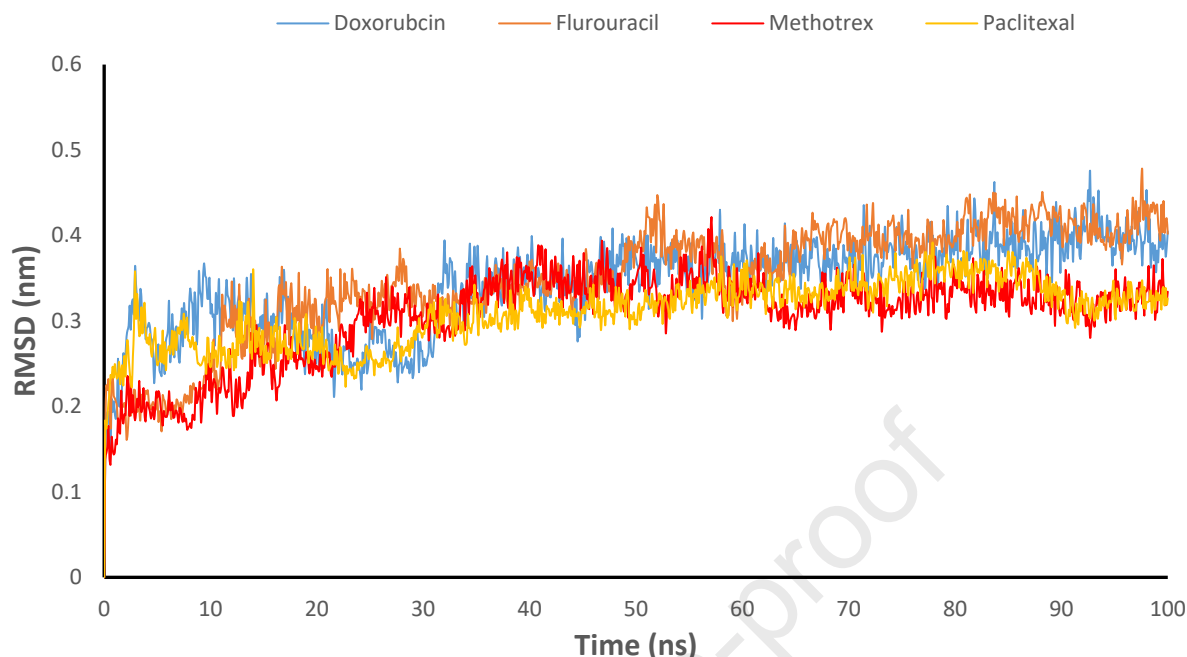


Figure 5 Trajectory of RMSD fit to backbone for the main protease of SARS-CoV-2 with 5-fluorouracil, doxorubicin, methotrexate and paclitaxel at 300 K

Root mean square fluctuation (RMSF) is very much similar to the RMSD in term of calculation. It is calculated using the coordinates of the individual amino acid residues. Conformational stability of amino acids of active cavity of main protease of SARS-CoV-2 can also be explained using RMSF. Fluctuation at particular region of amino acid can be correlated with molecular docking.^{49,50} Herein, RMSF analysis for the main protease of SARS-CoV-2 in presence of 5-fluorouracil, doxorubicin, methotrexate and paclitaxel were analyzed for 100 ns at 300 K as given in **Figure 6**. Fluctuation in the coordinates of the amino acid in region of 40-75, 130-145, 200-300 was recorded. These fluctuations can also be correlated to the particular docking result. In case of 5-fluorouracil, fluctuations are recorded in amino acid region of 130-160. In case of doxorubicin fluctuation recorded in amino acid region of 100-110, 150-160, and 290-300. In case of methotrexate it was in 20-30 and 40-70. In case of paclitaxel fluctuation was around 250-260, 90-110, and 150-160. From the result, major fluctuations recorded in that region where docking take place. So, it can be concluded that fluctuation value of each graph corroborates the successful molecular docking.

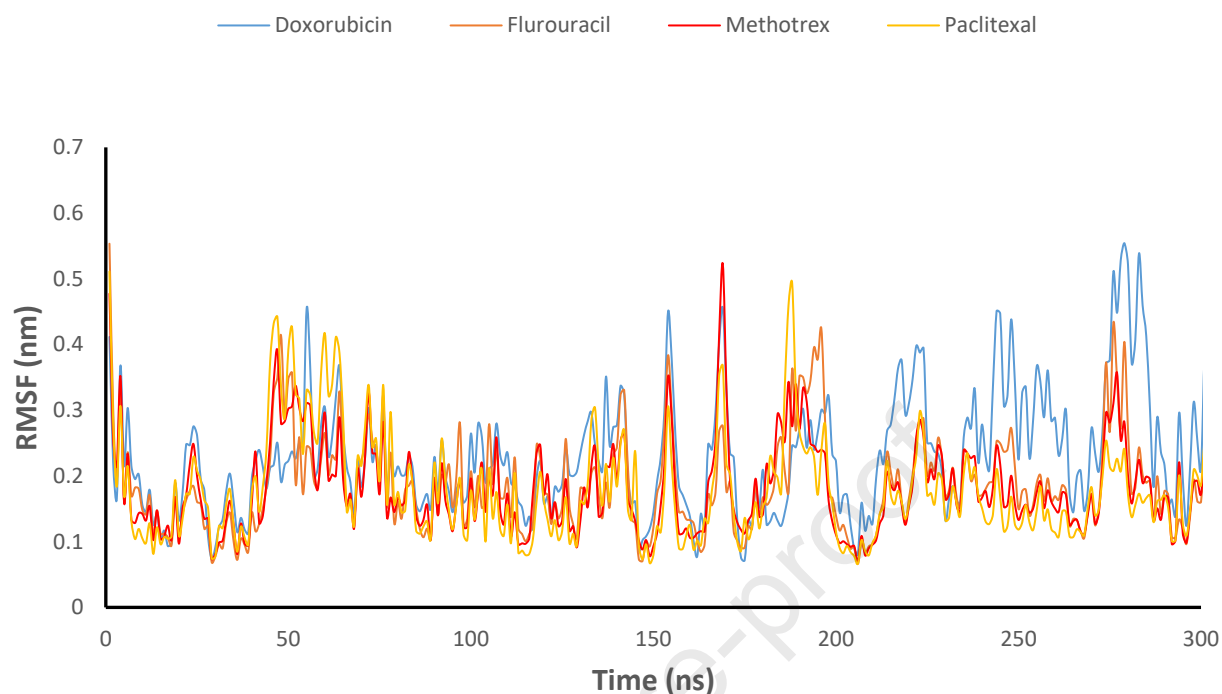


Figure 6 Trajectory of RMSF for the main protease of SARS-CoV-2 with 5-fluorouracil, doxorubicin, methotrexate and paclitaxel at 300 K

Hydrogen bonding interaction is the most important interaction in molecular docking analysis. Their stability during a time span can be analyzed by using molecular dynamics simulations. These interactions are of two types: conventional and non-conventional. Conventional hydrogen bonding is more important because it is strong and formed between hydrogen and most electronegative atoms. Non-conventional hydrogen bonds are formed by the other element (except F, N and O) with hydrogen. It is less important but play role in the anchoring of the ligand within the active binding cavity along with conventional hydrogen bonding. The overall binding is measured in term of several bonds with their length. Larger the number of hydrogen bonds and short length of hydrogen bonds, shows effective anchoring.⁵¹ Herein, hydrogen bonding analysis for the main protease of SARS-CoV-2 with 5-fluorouracil, doxorubicin, methotrexate and paclitaxel were analyzed for 100 ns at 300 K as given in **Figure 7**. 5-Fluorouracil, doxorubicin, methotrexate and paclitaxel forms maximum 4, 6, 7 and 5 hydrogen bonds. It was found that number of hydrogen bonds differs in molecular docking and MD simulation. It is due to that MD simulations consider both types of hydrogen bonding and during a simulation time, some of the bond break and some new bonds were formed.

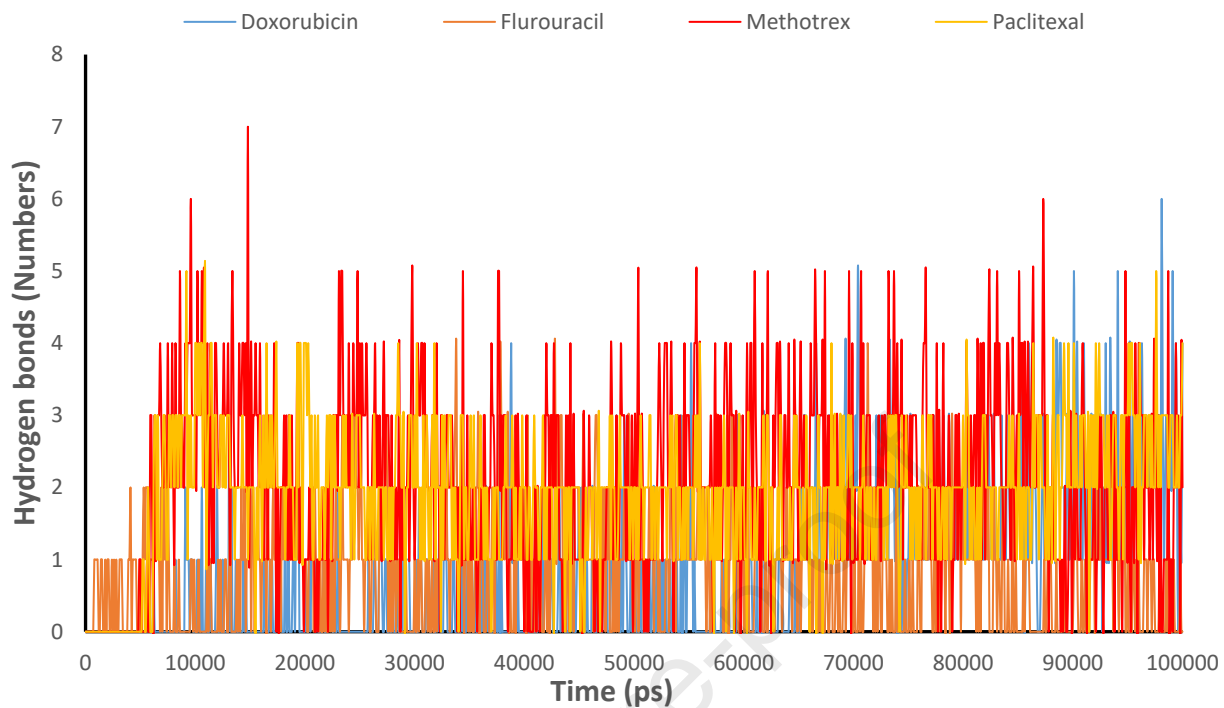
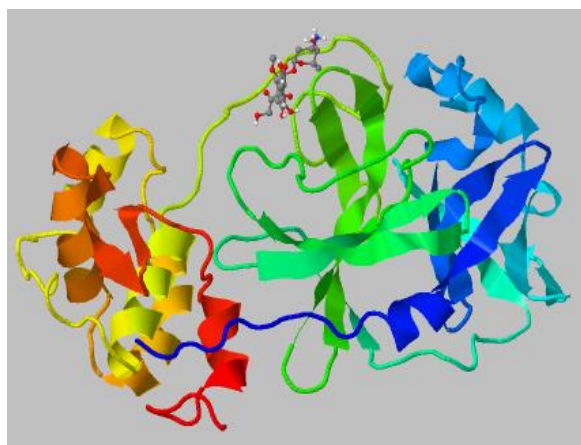


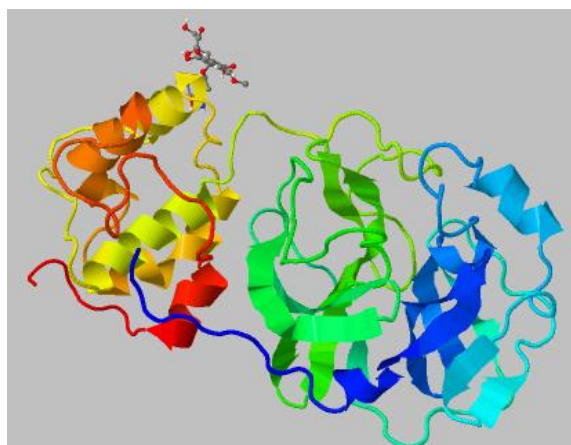
Figure 7 Trajectory hydrogen bond for the main protease of SARS-CoV-2 with 5-fluorouracil, doxorubicin, methotrexate and paclitaxel at 300 K

Temperature dependent MD simulations of Mrpo of nCoV with doxorubicin (290, 310, 320 and 325 K)

Herein temperature dependent MD simulation of doxorubicin with main protease of SARS-CoV-2 was performed to analyse the changes that occurred on temperature variation. **Figure 8** represent the docked view of Mpro of SARS-CoV-2 with Doxorubicin at 290, 310, 320 and 325 K.



290 K



310 K

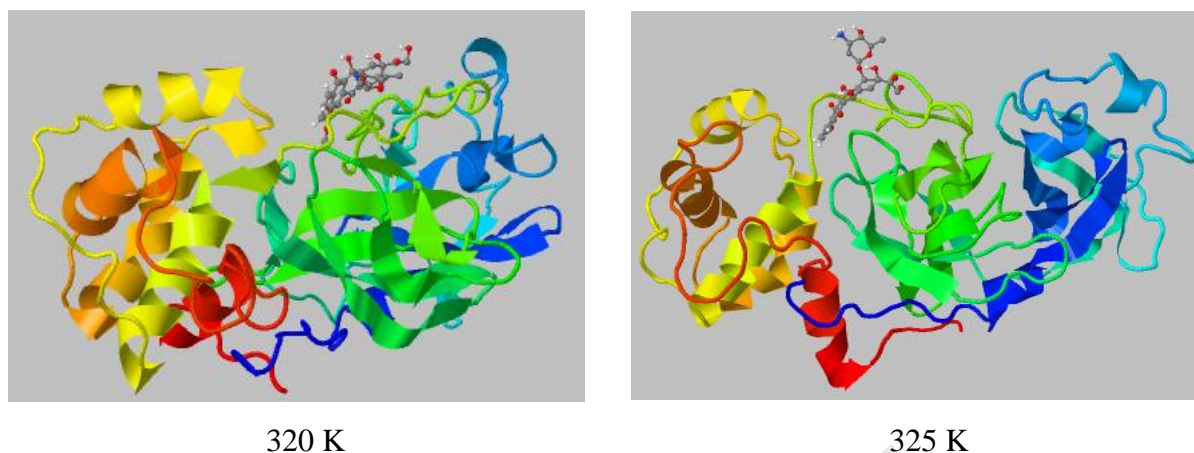


Figure 8 Docked view of Mpro of SARS-CoV-2 with doxorubicin at **290, 310, 320 and 325 K**

The distance from the center of mass of a body to the point at which the mass of the body might be concentrated without causing a change in its moment of rotational inertia around an axis that passes through the center of mass is referred to as the radius of gyration. It is used to define the stability of the protein ligand complex just like other parameters. The conformational changes in the macromolecules system occur when the ligand is driven to fit into the binding cavity. A smaller the value of Rg indicate more stability of complex.⁴³ **Figure 9** shows the result of analysed value of Rg for complex Mpro-nCov with doxorubicin at different temperature. From **Figure 9**, it is clear that at temperature 325 K Rg plot have less values and at temperature 310 K, the Rg plot have high values with less fluctuation. As a result, it is evident that at 290 K, the complex is more stable.

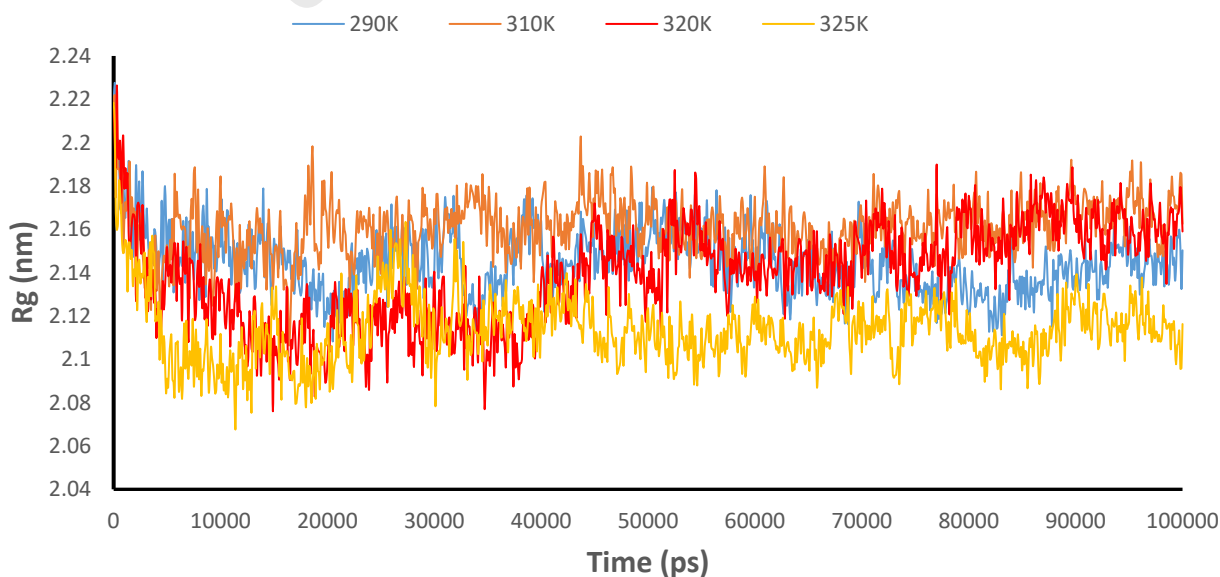


Figure 9 Trajectory of radius of gyration for the Mpro of SARS-CoV-2 with doxorubicin at **290, 310, 320 and 325 K**

The main protease of SARS-CoV-2 in presence of doxorubicin was examined for 100ns at 290, 310, 320 and 325 K as in **Figure 10**. At temperature 290 K and 310 K, RMSD values for doxorubicin were between 0.21 to 0.3nm whereas at 320 K and 325 K, the RMSD values for doxorubicin were in between 0.3 to 0.45nm. From **Figure10**, it is clear that at 320 K and 325 K, high fluctuations are observed and it indicates large conformational stability. At 290 K and 310 K, short change in RMSD values are observed and indicates stable complex formation. The overall finding shows that at 290 K the complex of main protease of SARS-CoV-2 with doxorubicin complex is most stable.

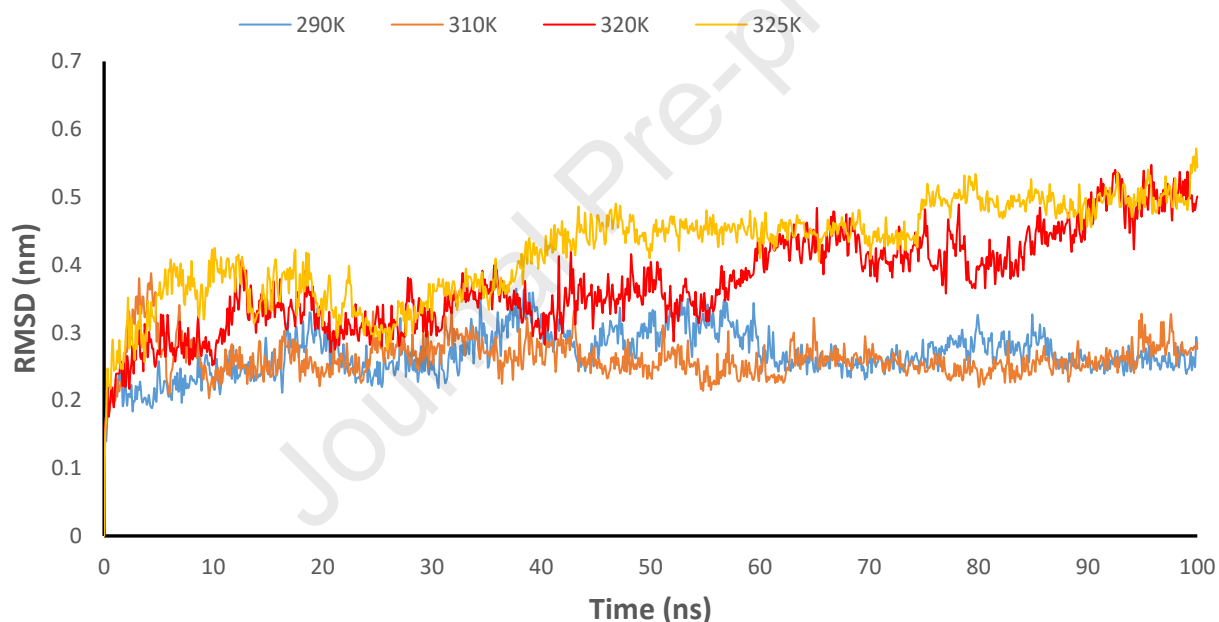


Figure 10 Trajectory of RMSD fit to backbone for the Mpro of SARS-CoV-2 with doxorubicin at **290, 310, 320 and 325 K**

Herein, RMSF was examined for the complex of main protease of SARS-CoV-2 with doxorubicin at 290 K, 310 K, 320 K and 325 K for 100 ns time span. (**Figure 11**) The amino acid coordinates fluctuated in the region 40-65, 130-145, 175-200, 240-265 and 270-290 and indicates docking area. At 290 K, fluctuation recorded in amino acid region of 50-70 and 180-200. At 310 K, fluctuation recorded in amino acid region of 50-75, 90-110 and 210-240. At 320 K fluctuation recorded in amino acid region of 40-70, 90-110 and 175-200. At 325 K, fluctuation recorded in

amino acid region of K 40-80, 90-110, 120-140 and 170-200. It is clear from the result that there are significant fluctuation in the area where docking occur. As a result, the value of each graph's fluctuation corroborates effective molecular docking. Least fluctuations are observed at 290 K, therefore, indicates the formation of most stable complex of Mpro of nCoV with doxorubicin for maximum inhibition.

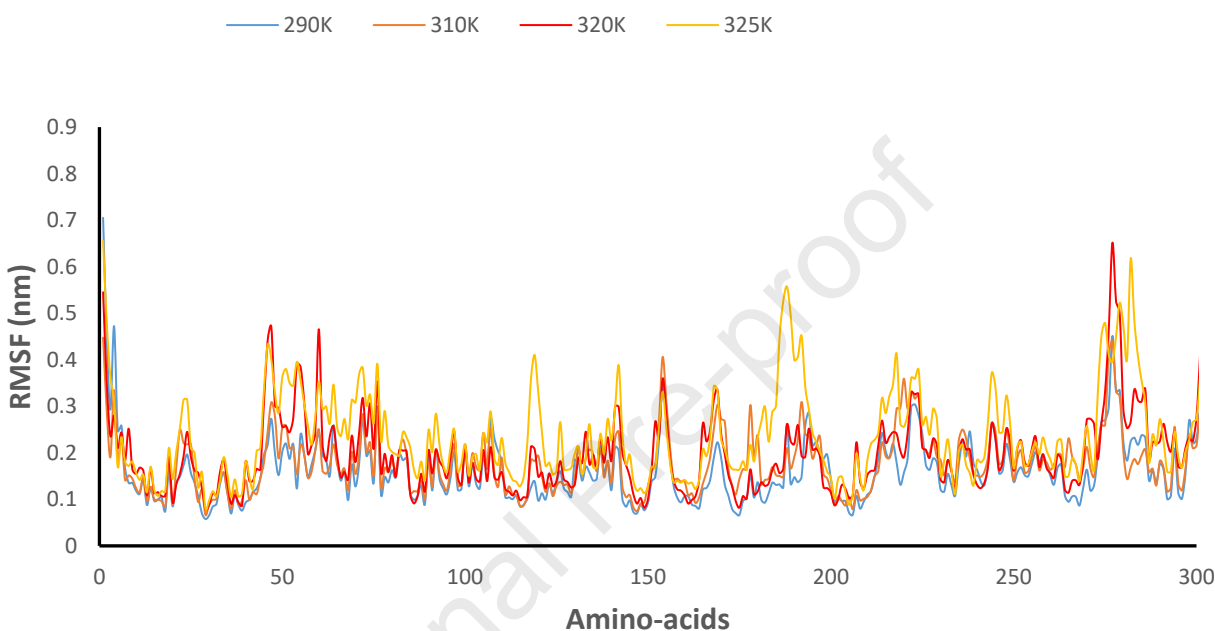


Figure 11 Trajectory of RMSF for the Mpro of SARS-CoV-2 with doxorubicin at **290, 310, 320 and 325 K**

The number of bonds and their lengths are used to determine the average number of a hydrogen bond. The anchoring is tighter as the number of hydrogen bond increases and the length of hydrogen bond decreases. **Figure12** shows the hydrogen bond study of main proteases of SARS-CoV-2 with doxorubicin at 290, 310, 320 and 325 K. At 290, 310, 320 and 325 K number of hydrogen bonds are 5, 4, 5 and 4 respectively. The number of hydrogen bonds gave an idea for the stability of the complex and other factors are also responsible to reach the conclusion for the stability of the formed complexes or the inhibition of Mpro of nCoV.

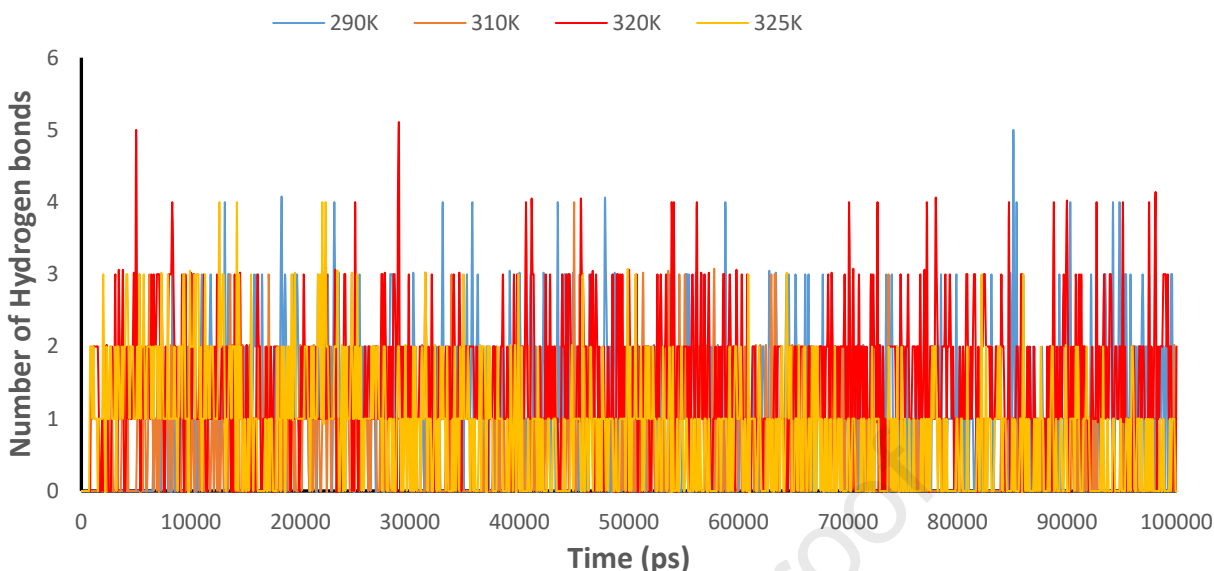
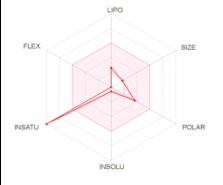
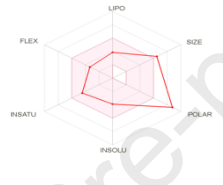
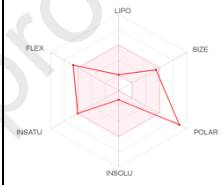
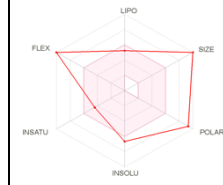


Figure 12 Trajectory of hydrogen bonds for the Mpro of SARS-CoV-2 with doxorubicin at **290, 310, 320 and 325 K**

ADME information

A molecule may be considered as a drug if it has the potential to reach its targeted place with enough concentration and must stay in a body for expected time to perform biological reaction. In drug development, ADME property considered to be important in the drug development.⁵² In this paper, a free web tool swissADME (<http://www.swissadme.ch>) has been used to predict different physiochemical and pharmacokinetics properties^{53,54} of 5-fluorouracil, doxorubicin, methotrexate and paclitaxel. Lipophilicity is one of the most important criteria to predict the molecule as a drug and it is a partition coefficient of n-octanol and water ($\log P_{O/W}$).⁵⁵⁻⁵⁷ The $\log_{O/W}$ value must be equal to less than 5 for effective drug. Hydrogen bond acceptor (HBA) and hydrogen bond donor (HBD) are also important factors for drug molecules and its values range is less than 5 for HBD and less than 10 for HBA.⁵⁸ Solubility is also one of an important parameter.^{59,60} The physiochemical data of 5-fluorouracil, doxorubicin, methotrexate and paclitaxel are given in **Table 3**.

Table 3. Physiochemical properties of all the four compounds

Physiochemical properties	5 Fluorouracil	Doxorubicin	Methotrexate	Paclitaxel
Log S	-0.58	-1.19	-1.19	-6.66
Solubility	Very soluble	Soluble	Very soluble	Soluble
Heavy atoms	9	39	33	62
Molecular weight (g/mol)	130.08	543.52	454.44	853.91
No. of rotational bonds	0	5	10	15
No. H-bond acceptors	3	12	9	14
Num. H-bond donors	2	6	5	4
Log $P_{o/w}$ (WLOGP)	-0.38	0.13	0.13	3.41
Physiochemical space for oral bioavailability				

For drug-likeness topological polar surface area (TPSA) is an important parameter and its value must be less than 130 Å for better result and online web server molinspiration (www.molinspiration.com) is used for TPSA determination. TPSA is thought to be a valuable measure for predicting drug transport abilities of compound.^{61,62} The TPSA should be in the range of 20 to 130 for excellent polarity. The screened compound doxorubicin, methotrexate and paclitaxel were not fall in this range except 5-fluorouracil having TPSA value 65.72 Å. Lipinski's rule of five is method for identifying substances with significant absorption aspect. The rule state that when a compound meets two or more of the following criteria then poor absorption or permeation is more likely: (i) the molecular weight exceeds 500 (ii) the log p value determined is more than five (iii) more than five hydrogen bond donor are present (iv) more than ten hydrogen bond acceptor are present.^{63,64,65} Most drugs in the blood cannot enter the brain because of the blood brain barrier (BBB). The existence of BBB some time raised a problem for development of brain illness drugs.⁶⁶ The permeability of GI mucosa as well as the movement rate along the GI tract may affect the GI absorption of orally administered medicines.^{67,68} The gastric emptying rate is widely recognised for influencing the plasma concentration profile of orally given medicines and intestinal transit rate. GI absorption for 5-fluorouracil is high while it is low for doxorubicin,

methotrexate and paclitaxel have low. 5-fluorouracil and methotrexate were follows Lipinski rule with allowed number of violations. (**Table 4**)

Table 4. Bioactivity and Drug likeness score of 5-fluorouracil, doxorubicin, methotrexate and paclitaxel

C. No.	GI absorption	BBB permeant	Lipinski	Log K _p (skin permeation) (cm/s)	TPSA (Å)	P-gp substrate
5 Fluorouracil	High	No	Yes; 0 violation	-7.73	65.72	No
Doxorubicin	Low	No	No; 3 violations: MW>500, NorO>10, NHorOH>5	-8.71	206.07	Yes
Methotrexate	Low	No	Yes; 1 violation: NorO>10	-10.39	210.54	Yes
Paclitaxel	Low	No	No; 2 violations: MW>500, NorO>10	-8.91	221.29	Yes

Conclusion

Herein, work authors chosen the repurposing drugs (5-fluorouracil, doxorubicin, methotrexate and paclitaxel) and docked them against main protease of SARS-CoV-2 using iGemdock. The docking results were quite significant. Binding energy of 5-fluorouracil, doxorubicin, methotrexate and paclitaxel against Mpro of nCoV are -74.5918, -121.89, -111.43, and -99.9097 kcal/mol respectively. Among them doxorubicin has lowest binding energy -121.89 kcal/mol i.e. showing promising interaction with the main protease of SARS-CoV-2 and the maximum inhibition. For more accurate and reliable results authors have performed MD simulations of all four compound with main protease of SARS-CoV-2 using WebGro at 300 K. MD simulations corroborates our docking results and the complex formed by doxorubicin is stable. Further temperature dependent MD simulations were also performed for main protease of SARS-CoV-2 with doxorubicin at 290, 310, 320 and 325 K to analyse changes that occurred in the complexes. It was found a most stable complex of Mpro of nCoV with doxorubicin was formed at 290 K. ADME properties were determined to check the solubility, bioavailability and potential of a molecule to become effective drug.

Statements and Declarations**Disclosure of potential conflicts of interest and informed consent**

“I, Prashant Singh (the Corresponding Author), declare that this manuscript is original, has not been published before and is not currently being considered for publication elsewhere. *“All authors contributed to the study conception, design, data collection and analysis. All the authors have commented on previous versions of the manuscript.* I further confirm that the order of authors listed in the manuscript has been approved by all of us. The authors also declare that they have no known competing financial interests or personal relationships that could have appeared to influence the work reported in this paper.

Funding There is no source of financial support to perform the work.

Research involving Human Participants and/or Animals It is declared that no human participants and/or animals are used in this work.

References

- (1) Azer, S. A. COVID-19: Pathophysiology, Diagnosis, Complications and Investigational Therapeutics. *New Microbes New Infect.* **2020**, *37*, 100738.
<https://doi.org/https://doi.org/10.1016/j.nmni.2020.100738>.
- (2) Parasher, A. COVID-19: Current Understanding of Its Pathophysiology, Clinical Presentation and Treatment. *Postgrad. Med. J.* **2021**, *97* (1147), 312 LP – 320.
<https://doi.org/10.1136/postgradmedj-2020-138577>.
- (3) Wang, B.; Li, R.; Lu, Z.; Huang, Y. Does Comorbidity Increase the Risk of Patients with COVID-19: Evidence from Meta-Analysis. *Aging (albany NY)* **2020**, *12* (7), 6049.
- (4) Bohn, M. K.; Hall, A.; Sepiashvili, L.; Jung, B.; Steele, S.; Adeli, K. Pathophysiology of COVID-19: Mechanisms Underlying Disease Severity and Progression. *Physiology* **2020**, *35* (5), 288–301. <https://doi.org/10.1152/physiol.00019.2020>.
- (5) Majmundar, N.; Ducruet, A.; Prakash, T.; Nanda, A.; Khandelwal, P. Incidence, Pathophysiology, and Impact of Coronavirus Disease 2019 (COVID-19) on Acute Ischemic Stroke. *World Neurosurg.* **2020**, *142*, 523–525.
<https://doi.org/https://doi.org/10.1016/j.wneu.2020.07.158>.
- (6) Hope, A. A.; Evering, T. H. Postacute Sequelae of Severe Acute Respiratory Syndrome Coronavirus 2 Infection. *Infect. Dis. Clin. North Am.* **2022**, *36* (2), 379–395.
<https://doi.org/https://doi.org/10.1016/j.idc.2022.02.004>.
- (7) Jin, Z.; Du, X.; Xu, Y.; Deng, Y.; Liu, M.; Zhao, Y.; Zhang, B.; Li, X.; Zhang, L.; Peng, C.; Duan, Y.; Yu, J.; Wang, L.; Yang, K.; Liu, F.; Jiang, R.; Yang, X.; You, T.; Liu, X.; Yang, X.; Bai, F.; Liu, H.; Liu, X.; Guddat, L. W.; Xu, W.; Xiao, G.; Qin, C.; Shi, Z.; Jiang, H.; Rao, Z.; Yang, H. Structure of Mpro from SARS-CoV-2 and Discovery of Its Inhibitors. *Nature* **2020**, *582* (7811), 289–293. <https://doi.org/10.1038/s41586-020-2223-y>.
- (8) Boschiero, M. N.; Duarte, A.; Palamim, C. V. C.; Alvarez, A. E.; Mauch, R. M.; Marson, F. A. L. Frequency of Respiratory Pathogens Other than SARS-CoV-2 Detected during COVID-19 Testing. *Diagn. Microbiol. Infect. Dis.* **2021**, 115576.

- <https://doi.org/https://doi.org/10.1016/j.diagmicrobio.2021.115576>.
- (9) Tan, S. Bin; Chiu-Shee, C.; Duarte, F. From SARS to COVID-19: Digital Infrastructures of Surveillance and Segregation in Exceptional Times. *Cities* **2021**, 103486. <https://doi.org/https://doi.org/10.1016/j.cities.2021.103486>.
- (10) Lagi, F.; Trevisan, S.; Piccica, M.; Graziani, L.; Basile, G.; Mencarini, J.; Borchi, B.; Menicacci, L.; Vaudo, M.; Scotti, V.; Fabbri, A.; Bandini, G.; Tozzetti, C.; Berni, A.; Aiezza, N.; Pestelli, G.; Turchi, V.; Pignone, A. M.; Poggesi, L.; Nozzoli, C.; Morettini, A.; Rossolini, G. M.; Bartoloni, A. Use of the FebriDx Point-of-Care Test for the Exclusion of SARS-CoV-2 Diagnosis in a Population with Acute Respiratory Infection during the Second (COVID-19) Wave in Italy. *Int. J. Infect. Dis.* **2021**, *108*, 231–236. <https://doi.org/https://doi.org/10.1016/j.ijid.2021.04.065>.
- (11) Khater, I.; Nassar, A. In Silico Molecular Docking Analysis for Repurposing Approved Antiviral Drugs against SARS-CoV-2 Main Protease. *Biochem. Biophys. Reports* **2021**, *27*, 101032. <https://doi.org/https://doi.org/10.1016/j.bbrep.2021.101032>.
- (12) Aronsky, I.; Masoudi-Sobhanzadeh, Y.; Cappuccio, A.; Zaslavsky, E. Advances in the Computational Landscape for Repurposed Drugs against COVID-19. *Drug Discov. Today* **2021**. <https://doi.org/https://doi.org/10.1016/j.drudis.2021.07.026>.
- (13) Vanhaelen, Q.; Mamoshina, P.; Aliper, A. M.; Artemov, A.; Lezhnina, K.; Ozerov, I.; Labat, I.; Zhavoronkov, A. Design of Efficient Computational Workflows for in Silico Drug Repurposing. *Drug Discov. Today* **2017**, *22* (2), 210–222. <https://doi.org/https://doi.org/10.1016/j.drudis.2016.09.019>.
- (14) Liu, J.; Zhai, Y.; Liang, L.; Zhu, D.; Zhao, Q.; Qiu, Y. Molecular Modeling Evaluation of the Binding Effect of Five Protease Inhibitors to COVID-19 Main Protease. *Chem. Phys.* **2021**, *542*, 111080. <https://doi.org/10.1016/j.chemphys.2020.111080>.
- (15) Marinho, E. M.; Batista de Andrade Neto, J.; Silva, J.; Rocha da Silva, C.; Cavalcanti, B. C.; Marinho, E. S.; Nobre Júnior, H. V. Virtual Screening Based on Molecular Docking of Possible Inhibitors of Covid-19 Main Protease. *Microb. Pathog.* **2020**, *148*, 104365. <https://doi.org/https://doi.org/10.1016/j.micpath.2020.104365>.

- (16) Zhang, Y. Protein Structure Prediction: When Is It Useful? *Curr. Opin. Struct. Biol.* **2009**, *19* (2), 145–155. <https://doi.org/10.1016/j.sbi.2009.02.005>.
- (17) Salmaso, V.; Moro, S. Bridging Molecular Docking to Molecular Dynamics in Exploring Ligand-Protein Recognition Process: An Overview. *Front. Pharmacol.* **2018**, *9*, 923. <https://doi.org/10.3389/fphar.2018.00923>.
- (18) Kuntz, I. D. Structure-Based Strategies for Drug Design and Discovery. *Science (80-.)*. **1992**, *257* (5073), 1078–1082. <https://doi.org/10.1126/science.257.5073.1078>.
- (19) Hollingsworth, S. A.; Dror, R. O. Molecular Dynamics Simulation for All. *Neuron* **2018**, *99* (6), 1129–1143. <https://doi.org/10.1016/j.neuron.2018.08.011>.
- (20) Longley, D. B.; Harkin, D. P.; Johnston, P. G. 5-Fluorouracil: Mechanisms of Action and Clinical Strategies. *Nat. Rev. Cancer* **2003**, *3* (5), 330–338. <https://doi.org/10.1038/nrc1074>.
- (21) Sharma, R.; Ashraf, R.; Kaur Gill, A.; Sharma, R. B. Design, Preparation and Evaluation of Nanoparticles of 5-Fluorouracil for the Targeted Delivery to Treat Colon Cancer. *Mater. Today Proc.* **2021**. <https://doi.org/10.1016/j.matpr.2021.09.200>.
- (22) Taymaz-Nikerel, H.; Karabekmez, M. E.; Eraslan, S.; Kırdar, B. Doxorubicin Induces an Extensive Transcriptional and Metabolic Rewiring in Yeast Cells. *Sci. Rep.* **2018**, *8* (1), 13672. <https://doi.org/10.1038/s41598-018-31939-9>.
- (23) Siani, P.; Donadoni, E.; Ferraro, L.; Re, F.; Di Valentin, C. Molecular Dynamics Simulations of Doxorubicin in Sphingomyelin-Based Lipid Membranes. *Biochim. Biophys. Acta - Biomembr.* **2022**, *1864* (1), 183763. <https://doi.org/10.1016/j.bbamem.2021.183763>.
- (24) Bar-On, O.; Shapira, M.; Hershko, D. D. Differential Effects of Doxorubicin Treatment on Cell Cycle Arrest and Skp2 Expression in Breast Cancer Cells. *Anticancer. Drugs* **2007**, *18* (10).
- (25) Huang, X.; Yan, H. Co-Administration of a Branched Arginine-Rich Polymer Enhances the Anti-Cancer Efficacy of Doxorubicin. *Colloids Surfaces B Biointerfaces* **2021**, *203*, 111752. <https://doi.org/10.1016/j.colsurfb.2021.111752>.

- (26) Friedman, B.; Cronstein, B. Methotrexate Mechanism in Treatment of Rheumatoid Arthritis. *Jt. Bone Spine* **2019**, *86* (3), 301–307.
<https://doi.org/https://doi.org/10.1016/j.jbspin.2018.07.004>.
- (27) Visser, K.; van der Heijde, D. Optimal Dosage and Route of Administration of Methotrexate in Rheumatoid Arthritis: A Systematic Review of the Literature. *Ann. Rheum. Dis.* **2009**, *68* (7), 1094–1099. <https://doi.org/10.1136/ard.2008.092668>.
- (28) Rowinsky, E. K.; Donehower, R. C. Paclitaxel (Taxol). *N. Engl. J. Med.* **1995**, *332* (15), 1004–1014. <https://doi.org/10.1056/NEJM199504133321507>.
- (29) Peltier, S.; Oger, J.-M.; Lagarce, F.; Couet, W.; Benoît, J.-P. Enhanced Oral Paclitaxel Bioavailability After Administration of Paclitaxel-Loaded Lipid Nanocapsules. *Pharm. Res.* **2006**, *23* (6), 1243–1250. <https://doi.org/10.1007/s11095-006-0022-2>.
- (30) Bernabeu, E.; Cagel, M.; Lagomarsino, E.; Moreton, M.; Chiappetta, D. A. Paclitaxel: What Has Been Done and the Challenges Remain Ahead. *Int. J. Pharm.* **2017**, *526* (1), 474–495. <https://doi.org/https://doi.org/10.1016/j.ijpharm.2017.05.016>.
- (31) Brown, T. ChemDraw. *Sci. Teach.* **2014**, *81* (2).
- (32) Bender, B. J.; Gahbauer, S.; Luttens, A.; Lyu, J.; Webb, C. M.; Stein, R. M.; Fink, E. A.; Balius, T. E.; Carlsson, J.; Irwin, J. J.; Shoichet, B. K. A Practical Guide to Large-Scale Docking. *Nat. Protoc.* **2021**, *16* (10), 4799–4832. <https://doi.org/10.1038/s41596-021-00597-z>.
- (33) Ugbe, F. A.; Shallangwa, G. A.; Uzairu, A.; Abdulkadir, I. Activity Modeling, Molecular Docking and Pharmacokinetic Studies of Some Boron-Pleuromutilins as Anti-Wolbachia Agents with Potential for Treatment of Filarial Diseases. *Chem. Data Collect.* **2021**, *36*, 100783. <https://doi.org/https://doi.org/10.1016/j.cdc.2021.100783>.
- (34) Burley, S. K.; Berman, H. M.; Kleywegt, G. J.; Markley, J. L.; Nakamura, H.; Velankar, S. Protein Data Bank (PDB): The Single Global Macromolecular Structure Archive. In *Protein Crystallography: Methods and Protocols*; Wlodawer, A., Dauter, Z., Jaskolski, M., Eds.; Springer New York: New York, NY, 2017; pp 627–641.
https://doi.org/10.1007/978-1-4939-7000-1_26.

- (35) Hsu, K.-C.; Chen, Y.-F.; Lin, S.-R.; Yang, J.-M. IGEMDOCK: A Graphical Environment of Enhancing GEMDOCK Using Pharmacological Interactions and Post-Screening Analysis. *BMC Bioinformatics* **2011**, *12* (1), S33. <https://doi.org/10.1186/1471-2105-12-S1-S33>.
- (36) Sarkar, B.; Ullah, M. A.; Araf, Y. A Systematic and Reverse Vaccinology Approach to Design Novel Subunit Vaccines against Dengue Virus Type-1 (DENV-1) and Human Papillomavirus-16 (HPV-16). *Informatics Med. Unlocked* **2020**, *19*, 100343. <https://doi.org/https://doi.org/10.1016/j.imu.2020.100343>.
- (37) Toor, H. G.; Banerjee, D. I.; Lipsa Rath, S.; Darji, S. A. Computational Drug Re-Purposing Targeting the Spike Glycoprotein of SARS-CoV-2 as an Effective Strategy to Neutralize COVID-19. *Eur. J. Pharmacol.* **2021**, *890*, 173720. <https://doi.org/https://doi.org/10.1016/j.ejphar.2020.173720>.
- (38) BEKKER, H.; BERENDSEN, H. J. C.; DIJKSTRA, E. J.; ACHTEROP, S.; VONDRUMEN, R.; VANDERSPOEL, D.; SIJBERS, A.; Keegstra, H.; RENARDUS, M. K. R. GROMACS - A PARALLEL COMPUTER FOR MOLECULAR-DYNAMICS SIMULATIONS; DeGroot, R. A., Nadrchal, J., Eds.; World Scientific Publishing; pp 252–256.
- (39) Abraham, M. J.; Murtola, T.; Schulz, R.; Páll, S.; Smith, J. C.; Hess, B.; Lindahl, E. Gromacs: High Performance Molecular Simulations through Multi-Level Parallelism from Laptops to Supercomputers. *SoftwareX* **2015**, *1–2*. <https://doi.org/10.1016/j.softx.2015.06.001>.
- (40) Lindorff-Larsen, K.; Piana, S.; Palmo, K.; Maragakis, P.; Klepeis, J. L.; Dror, R. O.; Shaw, D. E. Improved Side-Chain Torsion Potentials for the Amber Ff99SB Protein Force Field. *Proteins Struct. Funct. Bioinforma.* **2010**, *78* (8). <https://doi.org/10.1002/prot.22711>.
- (41) Lindahl, E.; Bjelkmar, P.; Larsson, P.; Cuendet, M. A.; Hess, B. Implementation of the Charmm Force Field in GROMACS: Analysis of Protein Stability Effects from Correction Maps, Virtual Interaction Sites, and Water Models. *J. Chem. Theory Comput.* **2010**, *6* (2). <https://doi.org/10.1021/ct900549r>.

- (42) Oostenbrink, C.; Villa, A.; Mark, A. E.; Van Gunsteren, W. F. A Biomolecular Force Field Based on the Free Enthalpy of Hydration and Solvation: The GROMOS Force-Field Parameter Sets 53A5 and 53A6. *J. Comput. Chem.* **2004**, *25* (13).
<https://doi.org/10.1002/jcc.20090>.
- (43) Vishvakarma, V. K.; Singh, P.; Kumar, V.; Kumari, K.; Patel, R.; Chandra, R. Pyrrolothiazolones as Potential Inhibitors for the NsP2B-NsP3 Protease of Dengue Virus and Their Mechanism of Synthesis. *ChemistrySelect* **2019**, *4* (32).
<https://doi.org/10.1002/slct.201901119>.
- (44) Kumar, D.; Kumari, K.; Jayaraj, A.; Kumar, V.; Kumar, R. V.; Dass, S. K.; Chandra, R.; Singh, P. Understanding the Binding Affinity of Noscipines with Protease of SARS-CoV-2 for COVID-19 Using MD Simulations at Different Temperatures. *J. Biomol. Struct. Dyn.* **2021**, *39* (7). <https://doi.org/10.1080/07391102.2020.1752310>.
- (45) Amin, S. A.; Ghosh, K.; Gayen, S.; Jha, T. Chemical-Informatics Approach to COVID-19 Drug Discovery: Monte Carlo Based QSAR, Virtual Screening and Molecular Docking Study of Some in-House Molecules as Papain-like Protease (PLpro) Inhibitors. *J. Biomol. Struct. Dyn.* **2021**, *39* (13), 4764–4773. <https://doi.org/10.1080/07391102.2020.1780946>.
- (46) Zhao, Y.; Zeng, C.; Massiah, M. A. Molecular Dynamics Simulation Reveals Insights into the Mechanism of Unfolding by the A130T/V Mutations within the MID1 Zinc-Binding Bbox1 Domain. *PLoS One* **2015**, *10* (4), 1–11.
<https://doi.org/10.1371/journal.pone.0124377>.
- (47) Schreiner, W.; Karch, R.; Knapp, B.; Ilieva, N. Relaxation Estimation of RMSD in Molecular Dynamics Immunosimulations. *Comput. Math. Methods Med.* **2012**, *2012*, 173521. <https://doi.org/10.1155/2012/173521>.
- (48) Zhang, D.; Lazim, R. Application of Conventional Molecular Dynamics Simulation in Evaluating the Stability of Apomyoglobin in Urea Solution. *Sci. Rep.* **2017**, *7* (1), 44651.
<https://doi.org/10.1038/srep44651>.
- (49) Picotti, P.; Marabotti, A.; Negro, A.; Musi, V.; Spolaore, B.; Zambonin, M.; Fontana, A. Modulation of the Structural Integrity of Helix F in Apomyoglobin by Single Amino Acid

- Replacements. *Protein Sci.* **2004**, *13* (6), 1572–1585.
<https://doi.org/https://doi.org/10.1110/ps.04635304>.
- (50) Lou, H.; Cukier, R. I. Molecular Dynamics of Apo-Adenylate Kinase: A Principal Component Analysis. *J. Phys. Chem. B* **2006**, *110* (25), 12796–12808.
<https://doi.org/10.1021/jp061976m>.
- (51) Kato, K.; Nakayoshi, T.; Fukuyoshi, S.; Kurimoto, E.; Oda, A. Validation of Molecular Dynamics Simulations for Prediction of Three-Dimensional Structures of Small Proteins. *Molecules* **2017**, *22* (10). <https://doi.org/10.3390/molecules22101716>.
- (52) Cannady, E.; Katyayan, K.; Patel, N. Chapter 3 - ADME Principles in Small Molecule Drug Discovery and Development: An Industrial Perspective. In *Haschek and Rousseaux's Handbook of Toxicologic Pathology (Fourth Edition)*; Haschek, W. M., Rousseaux, C. G., Wallig, M. A., Bolon, B., Eds.; Academic Press, 2022; pp 51–76.
<https://doi.org/https://doi.org/10.1016/B978-0-12-821044-4.00003-0>.
- (53) Prueksaritanont, T.; Tang, C. ADME of Biologics—What Have We Learned from Small Molecules? *AAPS J.* **2012**, *14* (3), 410–419. <https://doi.org/10.1208/s12248-012-9353-6>.
- (54) Daina, A.; Michielin, O.; Zoete, V. SwissADME: A Free Web Tool to Evaluate Pharmacokinetics, Drug-Likeness and Medicinal Chemistry Friendliness of Small Molecules. *Sci. Rep.* **2017**, *7* (1), 42717. <https://doi.org/10.1038/srep42717>.
- (55) Garrido, N. M.; Queimada, A. J.; Jorge, M.; Macedo, E. A.; Economou, I. G. 1-Octanol/Water Partition Coefficients of n-Alkanes from Molecular Simulations of Absolute Solvation Free Energies. *J. Chem. Theory Comput.* **2009**, *5* (9), 2436–2446.
<https://doi.org/10.1021/ct900214y>.
- (56) Daina, A.; Michielin, O.; Zoete, V. ILOGP: A Simple, Robust, and Efficient Description of n-Octanol/Water Partition Coefficient for Drug Design Using the GB/SA Approach. *J. Chem. Inf. Model.* **2014**, *54* (12), 3284–3301. <https://doi.org/10.1021/ci500467k>.
- (57) Tarcsay, Á.; Keserű, G. M. Contributions of Molecular Properties to Drug Promiscuity. *J. Med. Chem.* **2013**, *56* (5), 1789–1795. <https://doi.org/10.1021/jm301514n>.
- (58) Doak, B. C.; Over, B.; Giordanetto, F.; Kihlberg, J. Oral Druggable Space beyond the

- Rule of 5: Insights from Drugs and Clinical Candidates. *Chem. Biol.* **2014**, *21* (9), 1115–1142. <https://doi.org/https://doi.org/10.1016/j.chembiol.2014.08.013>.
- (59) Ritchie, T. J.; MacDonald, S. J. F.; Peace, S.; Pickett, S. D.; Luscombe, C. N. Increasing Small Molecule Drug Developability in Sub-Optimal Chemical Space. *Medchemcomm* **2013**, *4* (4), 673–680. <https://doi.org/10.1039/c3md00003f>.
- (60) Yilancioglu, K.; Weinstein, Z. B.; Meydan, C.; Akhmetov, A.; Toprak, I.; Durmaz, A.; Iossifov, I.; Kazan, H.; Roth, F. P.; Cokol, M. Target-Independent Prediction of Drug Synergies Using Only Drug Lipophilicity. *J. Chem. Inf. Model.* **2014**, *54* (8), 2286–2293. <https://doi.org/10.1021/ci500276x>.
- (61) Ertl, P.; Rohde, B.; Selzer, P. Fast Calculation of Molecular Polar Surface Area as a Sum of Fragment-Based Contributions and Its Application to the Prediction of Drug Transport Properties. *J. Med. Chem.* **2000**, *43* (20), 3714–3717. <https://doi.org/10.1021/jm000942e>.
- (62) Martin, Y. C. A Bioavailability Score. *J. Med. Chem.* **2005**, *48* (9), 3164–3170. <https://doi.org/10.1021/jm0492002>.
- (63) Ghose, A. K.; Viswanadhan, V. N.; Wendoloski, J. J. A Knowledge-Based Approach in Designing Combinatorial or Medicinal Chemistry Libraries for Drug Discovery. 1. A Qualitative and Quantitative Characterization of Known Drug Databases. *J. Comb. Chem.* **1999**, *1* (1), 55–68. <https://doi.org/10.1021/cc9800071>.
- (64) Egan, W. J.; Merz, Kenneth M.; Baldwin, J. J. Prediction of Drug Absorption Using Multivariate Statistics. *J. Med. Chem.* **2000**, *43* (21), 3867–3877. <https://doi.org/10.1021/jm000292e>.
- (65) Lipinski, C. A.; Lombardo, F.; Dominy, B. W.; Feeney, P. J. Experimental and Computational Approaches to Estimate Solubility and Permeability in Drug Discovery and Development Settings. *Adv. Drug Deliv. Rev.* **1997**, *23* (1), 3–25. [https://doi.org/https://doi.org/10.1016/S0169-409X\(96\)00423-1](https://doi.org/https://doi.org/10.1016/S0169-409X(96)00423-1).
- (66) Terasaki, T. Quantitative Expression of ADME Proteins at the Blood-Brain Barrier. *Drug Metab. Pharmacokinet.* **2017**, *32* (1, Supplement), S12. <https://doi.org/https://doi.org/10.1016/j.dmpk.2016.10.059>.

- (67) Kimura, T.; Higaki, K. Gastrointestinal Transit and Drug Absorption. *Biol. Pharm. Bull.* **2002**, *25* (2), 149–164. <https://doi.org/10.1248/bpb.25.149>.
- (68) Sawamoto, T.; Haruta, S.; Kurosaki, Y.; Higaki, K.; Kimura, T. Prediction of the Plasma Concentration Profiles of Orally Administered Drugs in Rats on the Basis of Gastrointestinal Transit Kinetics and Absorbability. *J. Pharm. Pharmacol.* **1997**, *49* (4), 450–457. <https://doi.org/10.1111/j.2042-7158.1997.tb06823.x>.

Journal Pre-proof